Proc. Indian Acad. Sci. (Earth Planet. Sci.), Vol. 97, No. 1, July 1988, pp. 21–34. © Printed in India.

# On the observed synoptic variability in the thermal structure of the upper northern Bay of Bengal during MONEX-79

R R RAO and BASIL MATHEW
Naval Physical and Oceanographic Laboratory, Cochin 682 004, India

MS received 8 June 1987; revised 25 February 1988

**Abstract.** The short-term variability observed in the near surface meteorological parameters and in the vertical thermal structure of the upper layers of the northern Bay of Bengal during a weak monsoonal regime is examined with the aid of time series measurements. The variability of the mixed layer depth is interpreted in terms of forced mixing caused by the surface wind stress and free mixing by buoyancy flux, Ekman pumping controlled by the curl of the surface wind stress, convergence associated with a clockwise gyral circulation and stratification caused by freshwater discharges from rivers. The daily-averaged current vectors in the upper layers indicate the presence of clockwise gyral circulation in the polygon area.

**Keywords.** Heat budget; thermal structure; mixed layer; heat content; clockwise gyre; synoptic variability.

## 1. Introduction

In the tropics, northern Bay of Bengal is a unique semi-enclosed basin experiencing seasonal reversing monsoons, depressions, severe cyclonic storms and consequently receives a large amount of rainfall and river run-off. The upper layers of the sea are therefore expected to respond to the hydrometeorological forcing through mass, momentum and heat inputs. Hence it is anticipated that the physical properties of the upper layers as temperature, salinity and currents would also exhibit large variability in the space-time domain. However, very few systematic investigations on the observed variability in the northern Bay of Bengal have been carried out, mainly due to paucity of data sets. Utilizing a variety of data sets, Wyrtki (1971), Colborn (1975), Hastenrath and Lamb (1979), Robinson *et al* (1979), Ramesh Babu and Sastry (1981) reported the seasonal variability of the thermal structure of the upper layers of the Bay of Bengal in the spatial domain. The corresponding information on the short-term variability is relatively meagre.

Prior understanding of the short-term variability in the thermal structure of the upper layers is extremely important in the fields of weather forecasting, fisheries exploration and underwater surveillance operations etc. Information on the thermal variability in the upper layers of the northern Bay of Bengal on the diurnal and synoptic scales is extremely sparse due to lack of systematic time series measurements. Fortunately the field measurement programmes of the recent summer monsoon experiments (MONSOON-77 and MONEX-79) conducted at selected stations over the northern Bay of Bengal afforded an unique opportunity to examine this problem in some detail for a limited period during the summer monsoon season. Rao *et al* (1981) utilizing MONSOON-77 data studied the observed synoptic scale variability in the

thermal structure of the upper layers over a limited area for one week preceding the formation of a monsoon depression. In another study, utilizing the bathythermograph (BT) data collected from an Indian ship, Rao *et al* (1983) described the upper oceanic thermal structure observed at selected stations in the northern Bay of Bengal for selective periods during May, June and July 1979 under the summer monsoonal forcing. In the present study an attempt was made to explain the observed short-term variability in the thermal structure of the upper layers of northern Bay of Bengal under a weak monsoonal regime utilizing time series data sets collected from USSR ships during MONEX-79.

## 2. Data

During 11 to 23 July 1979 four USSR ships formed a stationary polygon (figure 1) in the northern Bay of Bengal to monitor the characteristics of the upper air and upper ocean and to study the genesis and growth of monsoon depressions. Although no depression formed during this period, the collected data sets possibly provided some clues on the non-formation of any depression. Time series of all the standard marine meteorological elements including solar radiation were measured at hourly intervals. BT profiles provided six-hourly temperature data in the vertical upto about 200 m depth. These profiles usually contained data at 10 to 25 non-standard depths. However, as the BT data were not reported at standard depths, a cubic spline technique was adopted to generate data at every 5 m interval in the vertical below the mixed layer. Hydrocasts conducted at three-hourly interval provided salinity data except at the eastern location where the observational interval was 6 h. Daily averages or totals of meteorological and oceanographic elements were used in this study. In the following discussion the observational stations are designated as N, E, S and W corresponding to northern, eastern, southern and western locations of the polygon.

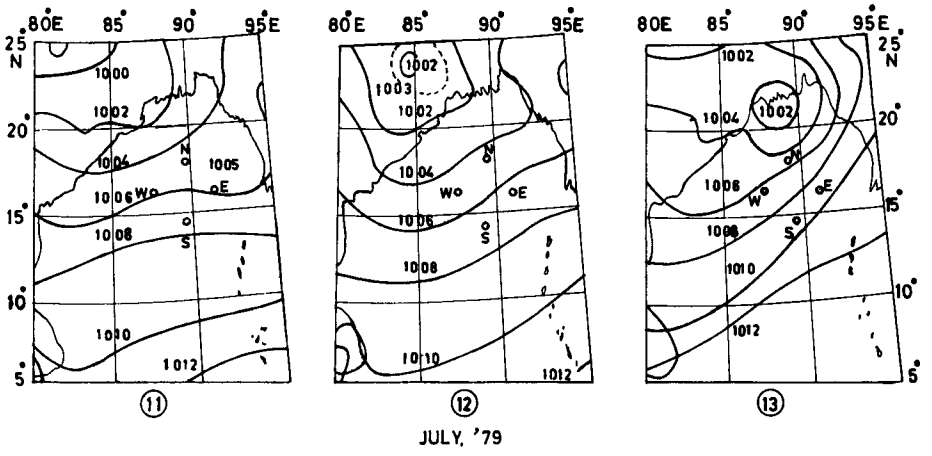


**Figure 1.** Station locations and daily surface pressure analysis from 11–13 July 1979 (contour interval 2 mb).

## 3. Weather

A brief summary of the weather extracted from Indian Daily Weather Reports is reported here. A low pressure area moved across the Arakan coast into northeastern Bay on 4 July and concentrated into a depression on 6 July. This depression crossed the coast on 8 July and moved west-northwest to the central parts of India by 10 July. By 15 July it moved as a low pressure area upto Rajasthan and merged with the seasonal low on 20 July. On 13 July, another low pressure area developed over the northern Bay (figure 1). It moved rapidly northwest on 14 July and merged with the monsoon trough over Bihar. With this the eastern end of the monsoon trough shifted northwards causing heavy rains over the foothills. The monsoon westerlies weakened resulting in weak monsoon conditions over the central parts of India. After this an east-west trough in lower and middle tropospheres formed across the sourthern peninsula on 21 July. This slowly shifted northwards and became well organised by 27 July when a low pressure area formed on its eastern end and moved westwards. At this stage the seasonal trough also shifted southwards and the low pressure area merged with it towards the end of July.

## 4. Results and discussion

To assess the role of heat exchange terms at the air-sea interface on the short-term variability of the SST and mixed layer depth (MLD) an attempt was made to budget these terms. The daily values of the observed meteorological parameters such as surface pressure (PR), scalar wind speed (FF), total cloud cover (TCL), dry bulb temperature (DB), dew point temperature (DP) and sea surface temperature (SST) utilized for heat budget computation are presented in figure 2. The heat budget equation

$$Q = Q_I + Q_L + Q_S + Q_E,$$

where $Q$ is the net ocean surface heat gain ($W/m^2$), $Q_I$ the net insolation after applying correction for albedo ($W/m^2$), $Q_L$ the net long wave radiation ($W/m^2$), $Q_S$ the sensible heat flux ($W/m^2$) and $Q_E$ the latent heat flux ($W/m^2$). The positive values indicate heat gain to the ocean. The $Q_I$ values were only measured directly while all the other terms were estimated (Rao *et al* 1985). The results are portrayed in figure 3. The $Q_I$ at the surface varied between 100 and 300 $W/m^2$ with the exception of N and E during the initial disturbed days, where the values were $< 50\,W/m^2$. Cloud cover was the most prominent element which influenced the short-term variability of $Q_I$. The day-to-day variation in cloud cover was reflected in $Q_I$. However, the correspondence may not be exact as the cloud cover was not measured with any instrument and hence may contain some subjective bias.

The net long wave radiation $Q_L$ was controlled by SST, moisture in the atmosphere and cloud cover. $Q_L$ did not exhibit strong variations but varied around $-42\,W/m^2$. $Q_S$, determined by air (at 10 m above sea surface) and sea temperature difference and the scalar wind speed, was almost negative throughout with relatively higher magnitude at N and E during initial disturbed period. The negative values imply heat loss to the ocean under the unstable regime. The highest value of $Q_S$ never exceeded $-30\,W/m^2$ even during the disturbed period. The values of $Q_E$, mostly governed by the near surface

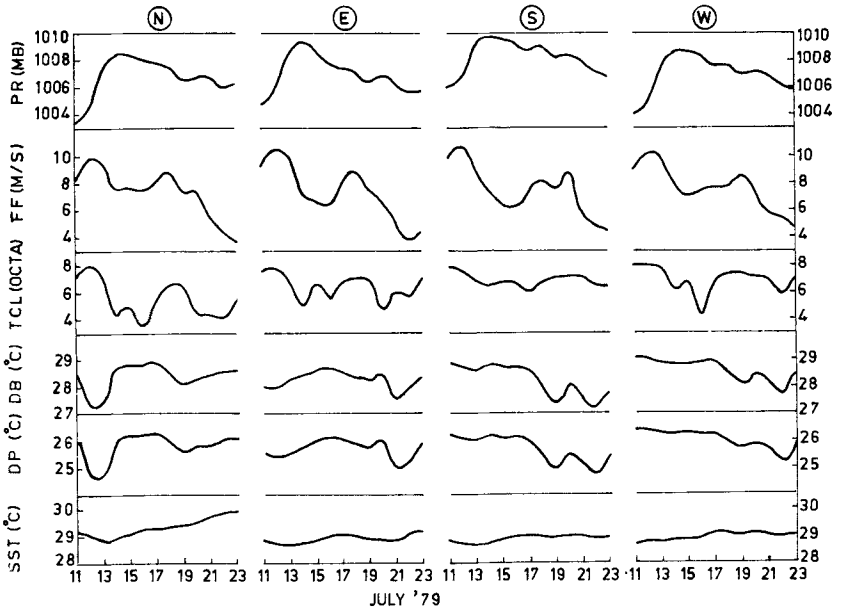


**Figure 2.** Daily march of surface meteorological parameters at the stationary locations.

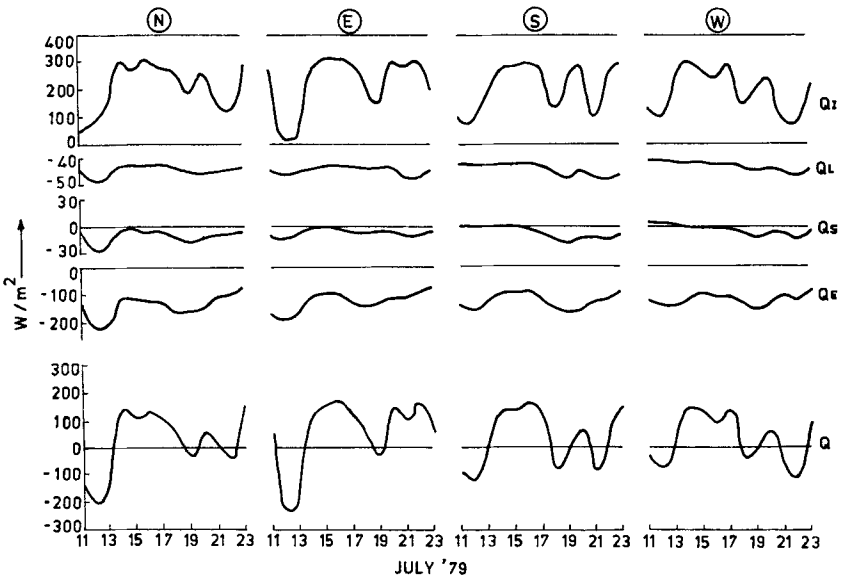


**Figure 3.** Daily march of surface heat budget estimates at the stationary locations.

vertical vapour pressure gradient and scalar wind speed ranged between $-100$ and $-200\ W/m^2$ and were higher during the initial disturbed period. A gradual decline in $Q_E$ is noticed at all the locations after the initial disturbed period. The balance between all these flux terms was denoted as the net oceanic heat gain $Q$. The distribution of $Q$ indicates depletion and accumulation of heat at the sea surface in alternate regimes. In general, large heat loss (about $-200\ W/m^2$) was noticed at N and E during the initial

disturbed period. The ocean mostly gained heat from 13/14 to 18 July 1979 at all the locations. Towards the end of the observational period the regime of $Q$ mostly fluctuated around zero line. In view of the absence of large fluctuations in the loss terms, the overall patterns of $Q$ and $Q_I$ resembled each other.

The synoptic scale variability in the near surface mixed layer depth (MLD) was governed by the forced mixing caused by wind and wave action and free mixing caused by buoyancy flux and Ekman pumping produced by the vertical component of curl of the surface wind stress under the stabilizing influence of stratified pycnocline below the mixed layer. An attempt was made to qualitatively relate the variability of MLD with these processes. Following Haney *et al* (1981) the forced mixing was represented by $U_*^3[U_* = (\tau/\rho_w)^{1/2}]$ where $U_*$ is the friction velocity, $\tau$ the surface wind stress and $\rho_w$ the density of mixed layer. The net heat gain/loss at the sea surface approximately corresponds to the buoyancy flux. The vertical component of the surface wind stress curl $(\nabla \times \tau)_z$ was estimated with the aid of wind data collected from the four ships. Here $(\nabla \times \tau)_z$ corresponds to the polygon area while $U_*^3$ and $Q$ correspond to the individual stations. The vertical density gradient (BLG) below the mixed layer was taken as a measure of stability. The daily march of these parameters is shown in figure 4. At all the locations there were strong vertical salinity gradients (figure 5), and the halocline was observed at shallower depths than the thermocline. Hence, MLD was determined from the daily averaged vertical profile of $\sigma_t[\sigma_t = (\rho_t - 1)\ 1000$, where $\rho_t$ is the in situ density]. The MLD was defined as the depth where $\sigma_t$ at sea surface $-0{\cdot}3\,\mathrm{kg\,m^{-3}}$ occurred in the daily averaged vertical $\sigma_t$ profile, which roughly correspond to the $\sigma_t$

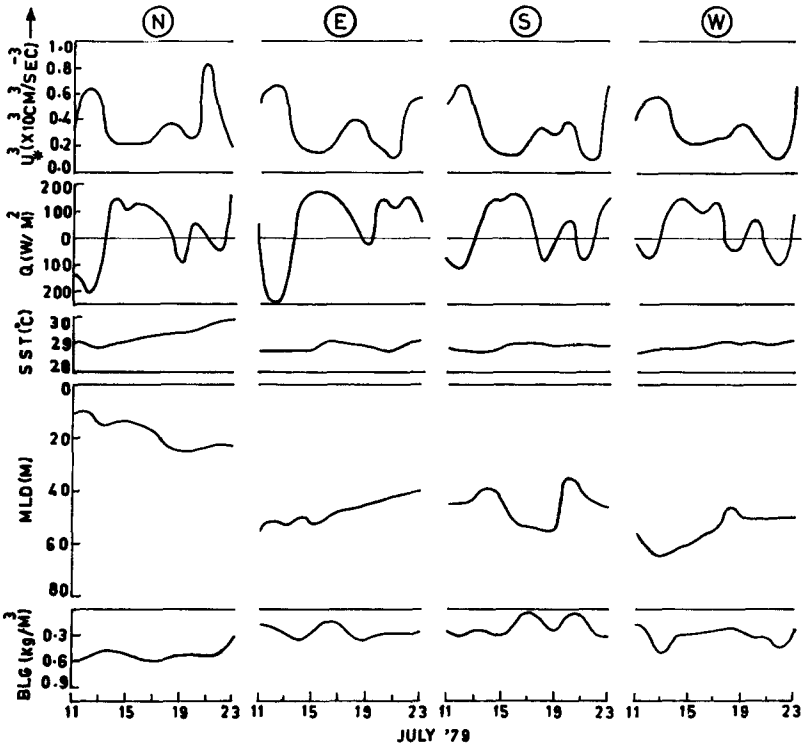


**Figure 4.** Daily march of $U_*$, $Q$, SST, MLD and BLG at the stationary locations.

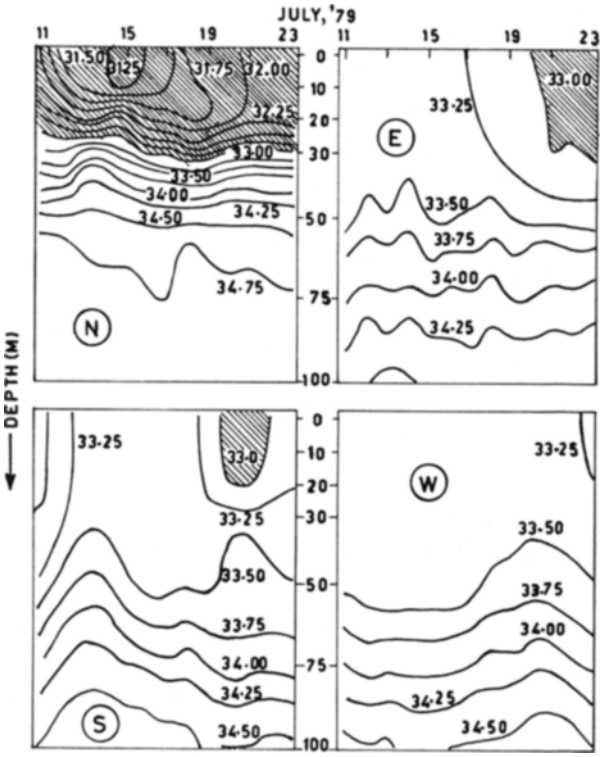


**Figure 5.** Daily averaged vertical salinity field at the stationary locations (contour interval 0·25‰).

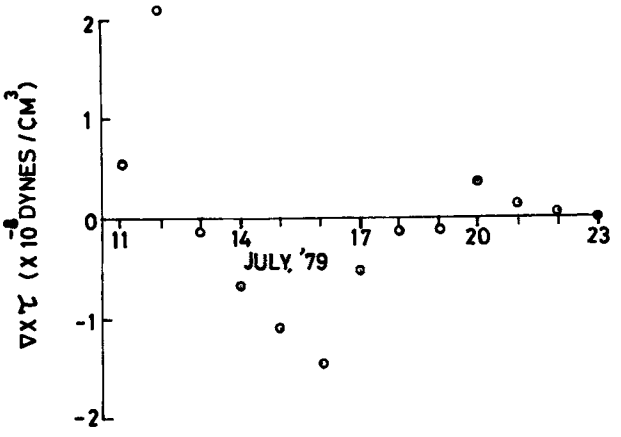


**Figure 6.** Daily march of vertical component curl of surface wind stress in the polygon area.

change associated with 1°C drop in the vertical thermal profile. In general MLD was relatively shallower at N and deeper at the other stations mainly due to the decrease in the bottom layer stratification away from the Head Bay. A strong halocline in the upper layers produced by the freshwater discharges from Ganges is responsible for the

**Table 1.**

| Location | Correlation between MLD and $U_*^3$ | Correlation between MLD and net heat gain |
|---|---|---|
| N | 0·12 | −0·17 |
| E | 0·17 | 0·42 |
| S | −0·09 | −0·15 |
| W | 0·26 | 0·21 |

meridional variation in BLG. For instance, BLG at N was almost double that of any other three stations (figure 4) where the freshwater influence was maximum. In general the mixed layer deepened at N, shoaled at E and W and was oscillatory at S. From the distribution of $\nabla \times \tau$ (figure 6) a shoaling tendency during initial period ($\nabla \times \tau < 0$) and deepening tendency thereafter until 19 July ($\nabla \times \tau > 0$) are to be anticipated in the MLD distribution. On the whole no such alternating trends were noticed in the MLD except at S. The $U_*^3$ was distinctly larger during the beginning and ending days at all the locations. Deepening rates of the layer should also be higher during these corresponding periods. However, no such one-to-one correspondence was noticed in the distribution of $U_*^3$ and MLD. The net heat gain was by and large negative only during the beginning and ending days (figure 3) and was positive at all the locations. The total heat gain varied between $0{\cdot}6 \times 10^8$ J/m$^2$ at E and $0{\cdot}18 \times 10^8$ J/m$^2$ at N. This type of heat accumulation lead to mixed layer shoaling. However, such a correspondence was noticed only at E and to a lesser extent at W. In order to obtain a more quantitative relationship between MLD and free and forced mixing the respective correlation coefficients were computed (table 1). At all locations the correlation between MLD and net heat gain was not significant with maximum value of 0·42 at E. The contribution of forced mixing also appears to be very less as evidenced by the correlation coefficient. Rao *et al* (1981) found a good relationship between MLD and net heat gain nearly in the same area in August 1977. However, they did not consider the influence of salinity which showed considerable changes with depth and also with time (Rao and Sanil Kumar 1988) during the observational period. At all the locations the isothermal layer was much deeper than the isohaline layer and the synoptic variations in the salinity field were more conspicuous than that of the thermal structure.

During July a clockwise gyral circulation was noticed in the northern Bay of Bengal (US Navy Atlas 1976). This clockwise circulation can also modify the topography of the mixed layer depth. The divergence pattern from the observed current vectors from four ships at different depths was estimated to identify any such relationship. The day-to-day variability of divergence is shown in figure 7. The positive values imply divergence which is noticed during the first few days only at 25 m and 50 m depths followed by a switchover to convergence showing an increasing tendency with time. However, no such switching-over was noticed at 100 m, 150 m and 200 m depths. From the same data set Swallow (1983) inferred a weak clockwise eddy 400–500 km across, centred near

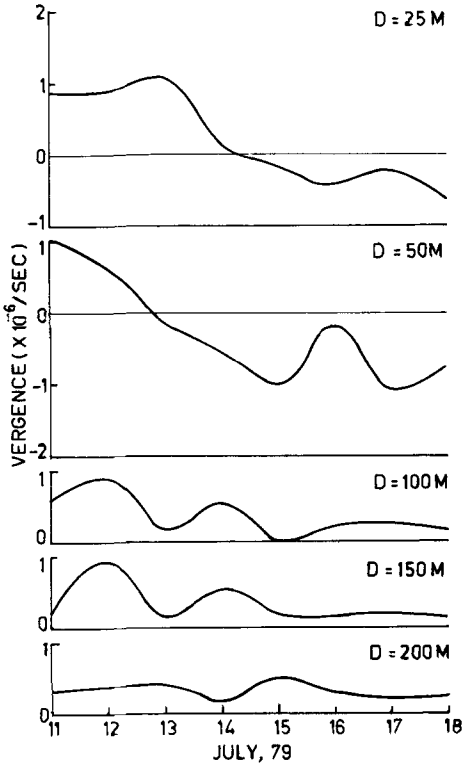


**Figure 7.** Daily march of divergence field in the polygon area.

14°N and 89°E where the 20°C isotherm was depressed 30 m. A clockwise eddy should result in convergence near its centre. However, no such anticipated deepening tendency of the mixed layer due to convergence was noticed at the S location. An attempt to link a possible relationship between the layer depth and current shear below the mixed layer did not yield positive results.

Though, during the observational period, the contribution of saltification/dilution caused by evaporation and rainfall was negligible in the polygon area (Rao and Sanil Kumar 1988), the salinity in the upper layers at all locations showed considerable variability (figure 5). The surface layer salinity at N showed a progressive decrease till 15 July and thereafter increased while at E and W a gradual fall was noticed throughout. At S the salinity increased till 16 July and showed an oscillatory nature thereafter. Since the contribution on salinity due to local evaporation/precipitation was negligible due to break monsoon conditions, advection seemed to be the only factor responsible for the considerable changes in the salinity regime. An increase/decrease in the freshwater discharge from Ganges and Brahmaputra rivers and its spreading into the four locations might have caused the observed variations in the salinity field. However, the variability observed in the salinity field was extremely difficult to parametrize due to lack of data on the time variation of river discharges and its resultant spreading into the observational area. It is interesting to note that the variability of MLD closely followed the salinity field at all the locations

except at N till 15 July (figures 4 and 5). The MLD at N showed a deepening tendency throughout, while the salinity in the upper layers decreased till 15 July and then increased. On the other hand the MLD at E and W shoaled where the salinity in the upper layers decreased. Both the MLD and the salinity field showed an oscillatory nature at S. Such close resemblence between the variability observed in MLD and salinity distribution probably implies that the MLD was governed by the stratification caused in the upper layers due to time-varying freshwater discharges into the Head Bay and its subsequent diffusion and circulation. Under a weak monsoonal spell, the influence of stratification caused by freshwater discharges seems to outweigh the contribution due to forced mixing, free mixing, Ekman pumping or divergence in regulating MLD in the polygon area.

The depth-time (daily-averaged) temperature fields drawn for all the four stations are shown in figure 8. Isotherms were drawn at 1°C interval by computer through linear interpolation. The presence of isothermal layer capped over stratified thermocline is evident at all the locations. The thickness of the isothermal layer was not of equal magnitude within the polygon area. Accumulation of heat within the mixed layer is clearly evident in the latter half of the observational period with the exception of W. The location and thickness of maximum vertical thermal gradient below mixed layer also differed within the polygon area. The phase-averaged distribution of this gradient will be discussed later to highlight this aspect. The short period waves might be viewed as the manifestation of inertial oscillations.

The phase-averaged BT profiles (11–23 July 1979) corresponding to the four stations (figure 9) clearly reveal the nature and magnitude of the horizontal variability prevailing in this area. The horizontal temperature differences in the top 30 m layer are insignificant. Below the isothermal layer the horizontal gradient was stronger in the north-south than that of in the east-west. Further, the gradient was not uniform in the vertical. For instance, in the north-south the temperature difference was over 5°C around 75 m depth and decreased on either side. This large spatial difference resulted mostly due to unequal mixed layer depths at the northern and southern locations.

The averaged profiles of the vertical thermal gradient for all the locations are shown in figure 10. Very weak gradients within the surface mixed layer are evident. Below this, the gradient gradually built up reaching a maximum in the depth range 90–120 m with the only exception N. At N the gradients sharply shot up reaching a peak value of 2·5°C/10 m around 45 m depth. The fall in the gradient below 45 m was less sharp compared to that reported above. At N, on the whole, the slab with $\partial T/\partial z > 1$°C/10 m persisted from 35 m to 85 m. Such a strong and thick stratified layer acts as an insulator for the vertical exchange of heat and salt. This would lead to trapping of the surplus heat energy in the mixed layer resulting in an anomalous increase of its heat content. The frequent formation of the meteorological disturbances during the summer monsoon season over the Head Bay of Bengal must therefore have some link with the growing mixed layer heat content. Rao *et al* (1981) reported such a possibility at this area during MONSOON-77. When the mixed layer heat content exceeds certain threshold limit it might infuse instability in the overlying monsoonal flow leading to the formation of a disturbance.

The daily march of the cyclonic heat potential ($HP_{28} = \rho C_p \int_0^{D_{28}} (T - 28)\,dz$) i.e. heat content with respect to 28°C where $D_{28}$ is the depth of 28°C and the heat content ($HC = \rho C_p \int_0^D T\,dz$) of the top 10 m, 100 m and 200 m layers is shown in figure 11. The $HP_{28}$ varied between 0·8 and 2·8 × $10^8$ J/m$^2$ with the highest horizontal differences

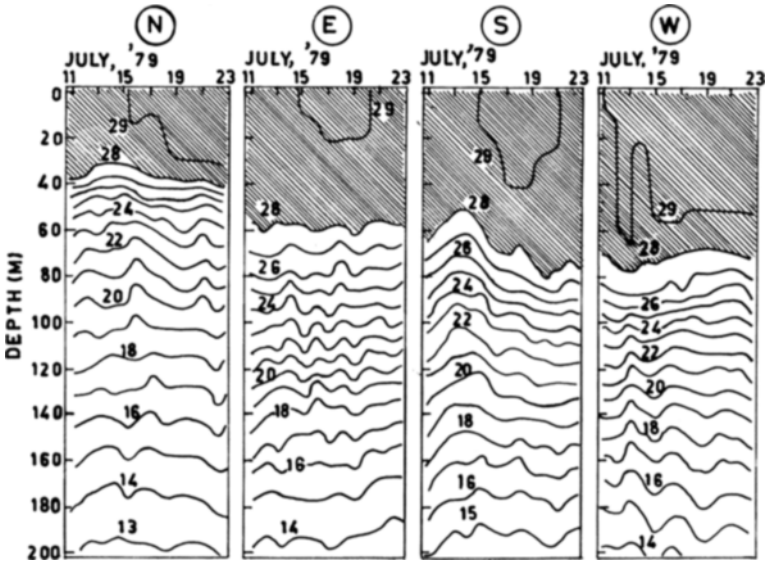


**Figure 8.** Daily averaged vertical temperature field at the stationary locations (contour interval 1°C).

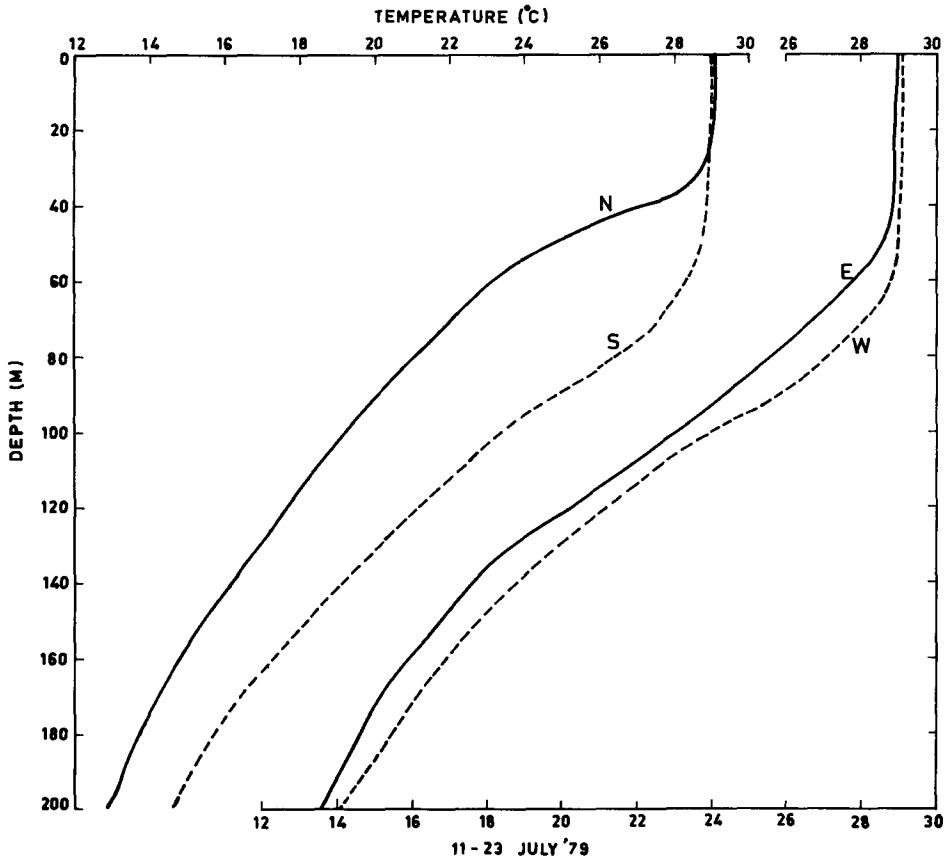


**Figure 9.** Phase averaged vertical temperature field at the stationary locations.

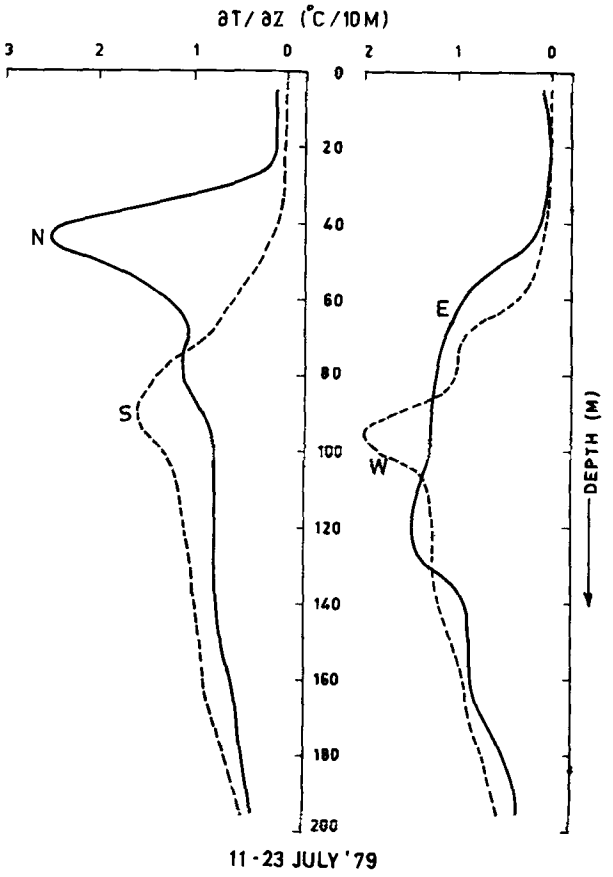


**Figure 10.** Phase averaged vertical temperature gradients at the stationary locations.

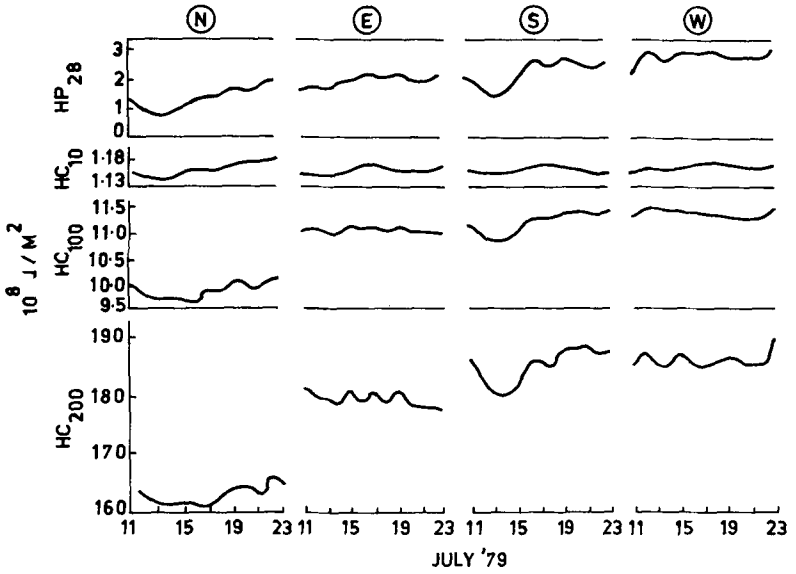


**Figure 11.** Daily march of cyclone heat potential ($HP_{28}$) and heat content with respect to 10, 100 and 200 m at stationary locations.

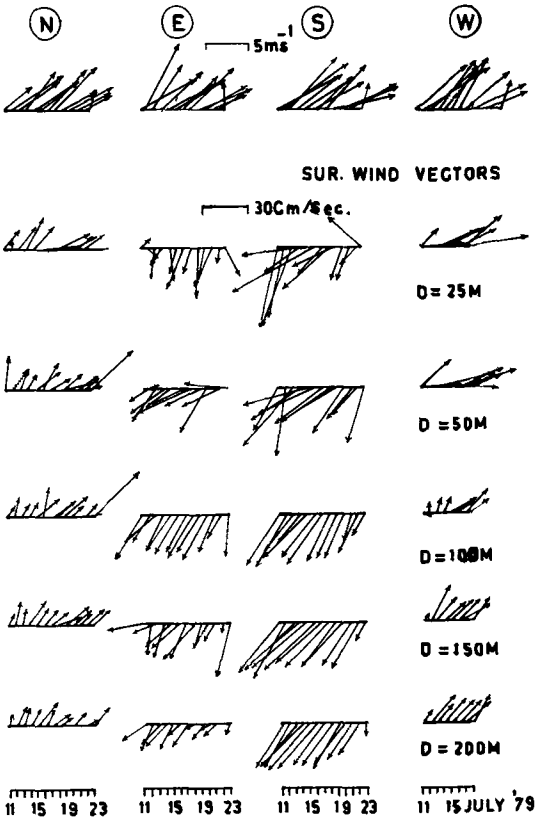


**Figure 12.** Daily averaged surface wind ($m\,s^{-1}$) and sub-surface current ($cm\,s^{-1}$) vectors at the stationary locations.

between N and W ($1{\cdot}2 \times 10^8\,J/m^2$). In general all the locations registered an increase of about $10^8\,J/m^2$ over this two-week period. This increase cannot be explained in terms of the surface heat flux alone (figure 4) but the contribution of advective heat is also to be considered. Evaporative heat loss at $-250\,W/m^2$, this area can sustain a meteorological disturbance for a 5-day period. The heat content pattern of the top 10 m layer roughly corresponded with that of SST. However, the heat content of the top 100 m and 200 m layers showed some interesting spatial variations. The lowest value of heat content prominent at N might be attributed to weak downward heat transfer on account of strong stratification caused by freshwater discharge. The temporal trends in heat content indicate increase/decrease of heat probably caused by baroclinic movement of the water in the upper thermocline.

The distribution of daily-averaged current vectors observed at standard depths for all the locations is shown in figure 12. In general the flow was towards northeast at N and W and towards southwest at E and S implying the presence of clockwise circulation in the polygon area. But the surface winds at all the locations were mostly from southwest with an average speed of 7 m/s. The observed circulation does not appear to be driven only by the local wind forcing. The strong spatial differences in the thermo-haline fields and the massive river discharges also appear to contribute to the circulation pattern. In

the presence of north-south thermal gradient heat advection may become important in the variability of the heat content of the layer. Warm water advection along the northwest limb and cold water advection along the southeast limb of the polygon is to be anticipated. This should result an increase in the heat content at N and a decrease at S. Observations support the speculation only for N and not for S. The increase of heat content at S may have to be viewed in terms of downward advection of heat probably caused by clockwise eddy circulation. The descent of isotherms (figure 9) and stronger currents throughout the top 200 m water column at S also favour this.

## 5. Conclusions

(i) As the monsoonal flow was mostly weak during the observational period (11–23 July 1979) fair weather conditions produced a mild heating in the surface layers due to net oceanic heat gain.

(ii) Mixed layer depth was minimum at the northern location compared to other locations due to stronger below layer stratification caused by freshwater river discharge. The day-to-day variability of MLD did not appear to have been controlled by forced and free mixing or Ekman pumping but seemed to have been influenced by stratification caused by the river discharges.

(iii) Analysis of the observed daily averaged current vectors indicated the presence of a clockwise eddy in the polygon area.

(iv) The horizontal thermal gradient in the upper thermocline was stronger in the north-south compared to that of east-west. Advection of heat in the horizontal and also in the vertical seems to have contributed to the observed increase in the heat content at the northern and southern stations respectively.

## Acknowledgement

Thanks are due to the Director, India MONEX Management Committee (IMMC), New Delhi, who made available all the data sets utilized in this study.

## Appendix

1. The daily averaged vertical component of surface wind stress curl $(\nabla \times \tau)_z$ was computed using the formula

$$(\nabla \times \tau)_z - \frac{\partial \tau_y}{\partial x} - \frac{\partial \tau_y}{\partial y}, \tag{1}$$

where $\tau = \rho_a C_D U^2$ in the surface wind stress (dynes $cm^{-2}$), $\tau_x$ the zonal component of $\tau$, $\tau_y$ the meridional component of $\tau$, $\rho_a$ the density of air (g/cc), $C_D$ the drag coefficient $1{\cdot}20 + 0{\cdot}00025\,U$ (Kondo 1975) and $U$ the daily averaged wind speed ($cm\,s^{-1}$).

2. The daily averaged divergence was computed using the formula

$$D = (\partial u/\partial x) + (\partial u/\partial y), \tag{2}$$

where $u$ and $v$ are the zonal and meridional components of daily averaged current ($cm\,s^{-1}$).

For numerical computation, the finite difference scheme is employed. Thus

$$(\Delta \times \tau)_z = \frac{\Delta \tau_y}{\Delta x} - \frac{\Delta \tau_x}{\Delta y}, \tag{3}$$

$$D = \frac{\Delta u}{\Delta x} + \frac{\Delta v}{\Delta y}, \tag{4}$$

where $\Delta x$ and $\Delta y$ are the geographical distance between stations in the zonal and meridional directions. Since the stations are located in the tropical belt, the correction due to convergence of meridians with latitude is ignored.

## References


Colborn J G 1975 *The thermal structure of the Indian Ocean. IIOE oceanographic monographs No. 2* (Honolulu: University Press) pp 173

Haney R L, Risch M S and Heise G C 1981 Wind forcing due to synoptic activity over the north Pacific Ocean; *Atmos. Ocean* **19** 128–147

Hanstenrath S and Lamb P J 1979 *Climate atlas of the Indian Ocean* (Wisconsin: University Press) Vols 1 and 2

Kondo J 1975 Air-sea bulk transfer coefficients in diabatic conditions; *Boundary-Layer Meteorol.* **9** 91–112

Ramesh Babu V and Sastry J S 1981 Heat storage in the Andaman Sea: *Mausam* **32** 145–150

Rao R R and Sanil Kumar K V 1988 Salinity variability in the upper layers of the Arabian Sea and Bay of Bengal during summer monsoon experiments (unpublished)

Rao R R, Gopalakrishna V V and Babu S V 1981 A case study on the northern Bay of Bengal sub-surface thermal structure and ocean mixed layer depth in relation to surface energy exchange processes during MONSOON-77; *Mausam* **32** 85–92

Rao R R, Rao D S, Murthy P G K and Joseph M X 1983 A preliminary investigation on the summer monsoonal forcing on the thermal structure of upper Bay of Bengal during MONEX-79; *Mausam* **34** 239–250

Rao R R, Ramam K V S, Rao D S and Joseph M X 1985 Surface heat budget estimates at selected areas of North Indian Ocean during MONSOON-77; *Mausam* **36** 21–32

Robinson M K, Bauer R A and Schroeder E H 1979 *Atlas of North Atlantic–Indian Ocean; monthly mean temperature and mean salinities of the surface layer.* Naval Oceanographic Office Reference Publication 18, Dept of the Navy (Washington DC) pp. 213

Swallow J C 1983 Eddies in the Indian Ocean: in *Eddies in marine science* (ed.) A R Robinson (Berlin: Springer-Verlag) p. 200

U S Navy 1976 *Marine climatic atlas of the world.* Vol III Indian Ocean (US Navy) pp. 348

Wyrtki K 1971 *Oceanographic atlas of the International Indian Ocean expedition* (Washington DC) pp. 531